

Reconstruction of Road Vehicle Wake by Physics Informed Neural Networks

Sanghyek Kim*, Jeoungmin Han, Junho Jeong, Yongsu Shin and Sanghyun Park

Aerodynamic Development Team
Hyundai Motor Group
150, HyundaiEonguso-ro, Namyang-eup
18280, Hwaseong-si, Gyeonggi-do, Korea
shkim0924@hyundai.com
hanjm@hyundai.com
jh.jeong@hyundai.com
shin.yongsu@hyundai.com
shpark@hyundai.com

Abstract: One of the ways to reduce the aerodynamic drag is by improving the rear wake of the vehicle. To achieve this, accurate measurements of flow velocity and pressure at the rear of the vehicle are essential. In the Hyundai Aero-Acoustic Wind Tunnel (HAWT), a wake measurement system with cobra probe arrays has been installed to measure and analyze the vehicle wake. However, the cobra probe can only properly detect the flows above 10m/s; thus, it cannot create an accurate wake contour within the range of -10m/s to 40m/s. In this paper, a Physics-Informed Neural Network (PINN) is applied to reconstruct the complete vehicle wake from this sparse data. The PINN model fills in the flow where velocities are below a certain threshold, allowing for a precise calculation of micro drag, a quantitative method for vehicle wake analysis. The generic aerodynamic model DrivAer, simulated via CFD, is used to validate the predictive accuracy of the PINN. As a result, the difference in aerodynamic drag coefficient between the ground truth and the PINN prediction is under 1 count ($\Delta C_D < 0.001$). Furthermore, the validated model was successfully applied to live wind tunnel data from the Hyundai IONIQ 5, enabling a quantitative diagnosis that guided a significant drag reduction. The application of PINN is expected to establish a more precise and practical technique for vehicle wake analysis.

1 Introduction

A detailed understanding of the flow field around a vehicle, which is shaped by its geometry and aerodynamic devices, is crucial for reducing aerodynamic drag. The Hyundai Aero-acoustic Wind Tunnel (HAWT) is equipped with a wake measurement system that employs Cobra Probes on an automated traversing system [1-2]. This setup allows for the real-time visualization and analysis of velocity and pressure fields in the vehicle's wake. However, a significant limitation of Cobra Probes, stemming from their structural design (see Section 2.1), is their inability to accurately measure reverse flow. This deficiency introduces distortions in the calculation of the Micro drag (see Section 2.2), a key metric for aerodynamic analysis.

Previous studies have attempted to overcome such data distortion issues arising from instrumentation limits. For instance, J.Jeong et al. applied a Deep Neural Network (DNN) to reconstruct missing data in the temperature field of a flat plate [3]. This work, however, was limited to thermal conduction, a phenomenon significantly less complex and more linear than a turbulent flow field. In another study, D. Kim et al. used an Adaptive Neuro Fuzzy Inference System(ANFIS) to predict the unmeasurable areas in the wake of a side mirror [4]. While successful, the study did not provide a clear rationale for how the ANFIS model learned the underlying physics of the flow.

To address these gaps, this paper introduces Physics-Informed Neural Networks (PINNs) to predict the flow data within the measurable regions of the vehicle wake [5]. By integrating the governing physical equations directly into its loss function, PINNs can learn the flow phenomena in a physically consistent manner. To validate our approach, we evaluate the prediction accuracy of the PINNs using CFD simulation data and benchmark its performance against a standard physics-uninformed neural network. Finally, we employ the Micro drag technique to assess the PINN's predictive accuracy and to perform a quantitative analysis of the complete flow field that results from augmenting the experimental data with the PINN's predictions.

2 Backgrounds

2.1 Cobra probe

The Cobra probe is an instrument designed for flow field measurement. Its operating principle, illustrated in Fig.1, involves measuring pressures at multiple holes on the probe head and then using the pressure differences to calculate the flow direction and three-dimensional velocity components. At HAWT, a 4-hole Fast Response Aerodynamic Probe (FRAP) from Vectoflow GmbH (Germany) is employed. This probe offers high-fidelity data acquisition, capturing pressure and velocity components in real-time at frequencies up to 2kHz.

Despite its capabilities, the Cobra probe has notable limitations. First, as an intrusive instrument (Fig.1), it inevitably disturbs the local flow field it is intended to measure. Second, its four-hole design restricts its effective measurement range to an acceptance angle of ± 45 degrees from its central axis. Finally, being a pressure-based sensor, its accuracy significantly degrades at low velocities, particularly below ~ 10 m/s.

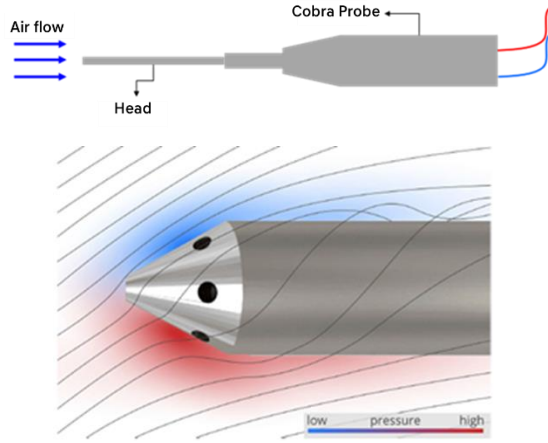


Figure 1: Multi-hole Cobra probe
(Source : vectoflow.de)

2.2 Micro Drag

Micro drag is an analytical technique, originally introduced by Cogotti, for diagnosing the sources of drag in a vehicle's wake [6]. The method is fundamentally based on the Reynolds Transport Theorem and works by calculating the momentum deficit in the flow as it traverses a specified control volume (see Eq.1)

$$C_D \cdot A_x = \int 1 - C_{p,tot} ds - \int \left(1 - \frac{u}{u_\infty}\right)^2 ds + \int \left(\left(\frac{v}{u_\infty}\right)^2 + \left(\frac{w}{u_\infty}\right)^2\right) ds \quad (1)$$

Where C_D is the drag coefficient acting on the vehicle, A_x is the frontal projected area of the vehicle, and $C_{p,tot}$ is the total pressure coefficient calculated from the flow passing through the control surface. u_∞ represents the freestream velocity in the wind tunnel, which corresponds to the driving speed in on-road conditions. The terms u, v , and w are the velocity components in the x, y , and z directions at the measurement points, respectively, and s denotes the control surface.

A primary output of this technique is a Drag map (Fig.2), which provides a visual and quantitative breakdown of how different areas in the wake contribute to the total aerodynamic drag. This allows engineers to pinpoint which flow structures are most responsible for increasing drag. The reliability of this powerful diagnostic tool, however, is critically dependent on the precise measurement of reverse flow regions. This exposes a key limitation in the current experimental setup at HAWT, where the Cobra probe's inability to measure reverse flow undermines the accuracy of the Micro drag analysis.

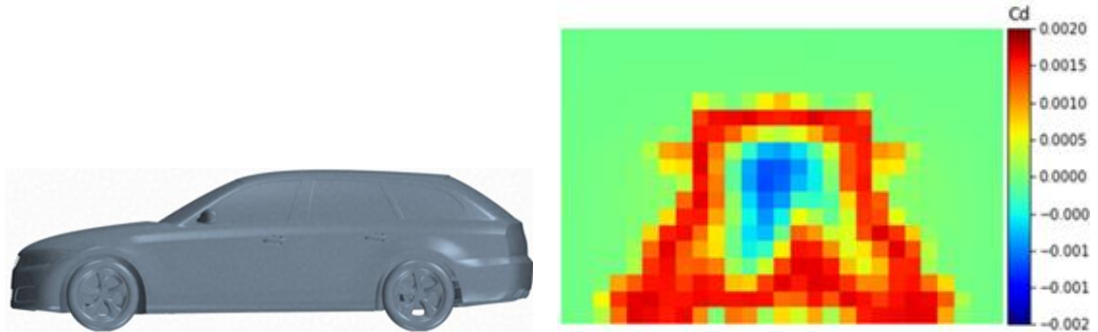


Figure 2: DrivAer Estate Model & Drag map

2.3 Physics Informed Neural Networks

Physics-Informed Neural Networks (PINNs), introduced by Raissi et al., represent a paradigm shift from traditional data-driven models [5]. While conventional neural networks learn exclusively from data, often ignoring the underlying physics, PINNs embed governing physical laws directly into the learning process. This is achieved by formulating a loss function that penalizes predictions for violating these laws, which not only reduces the reliance on large datasets but also accelerates model convergence.

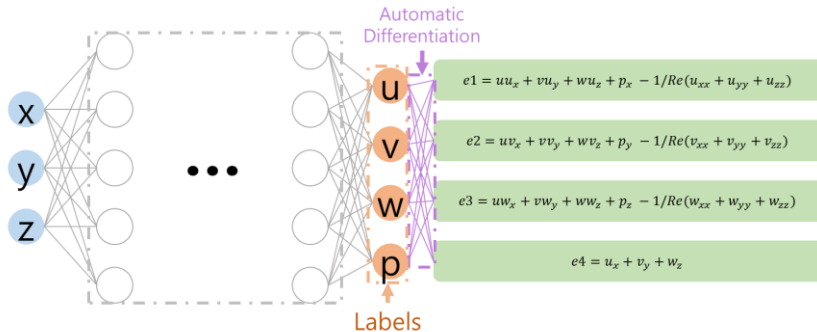


Figure 3: PINNs Architecture

The PINNs architecture, depicted in Fig.3, consists of two primary components. The first is a standard neural network that learns from available data points (left side). The second, and defining, component is the physics-informed part (right side), where the governing equations of fluid dynamics—the Navier-Stokes and Continuity equations—are formulated as a residual term in the loss function. This dual-objective training effectively constrains the solution space, preventing the network from producing physically implausible outcomes.

The model's total loss function L_{model} is therefore a composite of the data loss (L_{data}) and the physics loss ($L_{physics}$), as formulated in Eq.2. A powerful feature of this framework is that L_{data} and $L_{physics}$ need not be evaluated at the same spatial points. This allows the network to make accurate predictions even in regions devoid of measurement data by leveraging the physical laws learned from randomly sampled collocation points throughout the domain, alongside sparse information from actual sensor locations.

$$L_{model} = L_{data} + L_{physics} \quad (2)$$

Building on these capabilities, this study employs PINNs to address the measurement limitations of the Cobra Probe. Specifically, we leverage 1) the enforcement of physical laws and 2) the ability to predict in data-sparse regions to reconstruct the low-velocity airflow ($\leq 10\text{m/s}$) in the vehicle's wake. This reconstructed flow field is used to perform a quantitative aerodynamic analysis using the Micro drag technique.

3 Model Construction and Validation

This study validates the PINN's predictive capabilities using a semi-synthetic dataset derived from a high-fidelity CFD simulation of the DrivAer Estate model, a widely recognized benchmark in automotive aerodynamics [7]. To mimic the constraints of a real-world experiment, the complete CFD flow field was down-sampled to match the spatial resolution of the HAWT's wake measurement system. The resulting data, which forms the basis for our model training and validation, is shown in Fig.4.

The dataset is defined on a yz cross-sectional plane measuring 2.6m in width and 1.45m in height, situated 0.5m downstream from the vehicle's rear end. The data was partitioned for training and validation as follows:

- Training Data (for L_{data}): The data-driven loss component was trained on points from the “measurable” region, defined as where the axial velocity $u > 10\text{m/s}$. The inputs for the network were the spatial coordinates of these points, while the corresponding labels were the ground-truth velocity components (u, v, w) and pressure (p) from the CFD simulation.
- Collocation Points (for L_{physics}): The physics-informed loss component was enforced at collocation points sampled from the “unmeasurable” region ($u \leq 10\text{m/s}$). The loss at these points was calculated based on the residuals of the governing physical equations, which are detailed in the subsequent section.
- Validation Data: To quantitatively assess the model’s accuracy in the target region, a validation set was created using the data points where $u \leq 10\text{m/s}$. The inputs were the coordinates of these points, and the labels were their true velocity and pressure values from the CFD simulation, serving as the ground truth.

Figure 5 visualizes the initial training data, showing the u , v , and w velocity fields with the target prediction region ($u \leq 10\text{m/s}$) masked out.

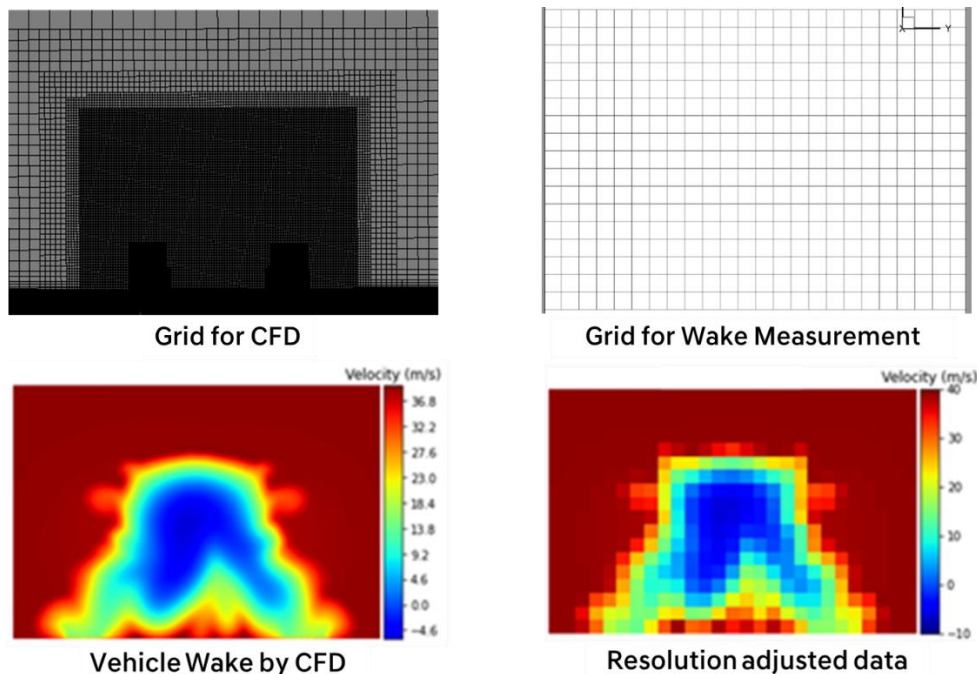


Figure 4. Down-sampling of CFD Wake results

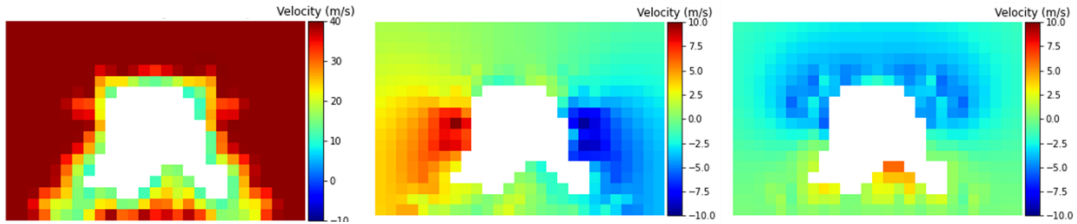


Figure 5. u, v, w velocity flow fields except unmeasurable region

3.1 Hyperparameter tuning

To optimize the model's predictive performance a two-stage tuning process was conducted: first on the neural network architecture, and second on the formulation of the physics-informed loss, L_{physics} . Other fundamental hyperparameters were kept constant as detailed in Table 1.

Table 1. Hyperparameter settings for PINN model

Hyperparameter	Value
Activation function	Tanh
Epochs	15,000
Batch size	5,000
Learning rate	1.0e-4

Network Architecture Optimization:

Optimizing the number of layers and neurons is essential for preventing common training pitfalls like overfitting and convergence to poor local minima. For this stage, we used a standard L_{physics} for formulation consisting of the coupled continuity equation (CE) and Navier-Stokes equations (NSE). We evaluated three distinct network architectures, comparing their performance based on the Mean Squared Error (MSE) calculated on the validation data from the unmeasurable region. The results are presented in Table 2

The architecture with 5 hidden layers with 50 neurons each achieved the best performance, exhibiting the lowest MSE. The deepest model (10 layers, 100 neurons) did not overfit within 15,000 epochs but seemed to get trapped in a local minimum. In contrast, the simplest model (5 layers, 10 neurons) was likely too shallow, lacking expressive capacity to accurately model the complex flow field, which resulted in a higher MSE.

Table 2. Results of Network architecture optimization

# of layers	# of neurons	MSE
5	10	0.27
5	50	0.16
10	100	0.36

Physics-Informed Loss (L_{physics}) Formulation:

In conventional machine learning, the loss function is not considered a hyperparameter. However, for PINNs, the selection of physical laws that constitute L_{physics} is a critical design choice that can significantly impact accuracy. The canonical choice for fluid dynamics is the coupled NSE and CE. To potentially enhance the physical consistency of the predictions, we investigated the effect of adding a third equation: the Pressure Poisson Equation (PPE). The PPE, derived by taking the divergence of the NSE, acts as a supplementary constraint that reinforces the mathematical compatibility between the pressure and velocity fields. We therefore constructed and compared several cases, each with a different combination of the three governing equations (formulated in Eq.3) and evaluated their performance based on the MSE in the unmeasurable region, as outlined in Table3.

(Navier-Stokes Equation) [8]

$$e1 = -\vec{u} \cdot \nabla \vec{u} - \frac{\nabla p}{\rho} + \mu \nabla^2 \vec{u}$$

(Continuity Equation) [8]

$$e2 = \nabla \cdot \vec{u} \quad (3)$$

(Pressure Poisson Equation) [8]

$$e3 = \nabla \cdot (-\vec{u} \cdot \nabla \vec{u} - \frac{\nabla p}{\rho} + \mu \nabla^2 \vec{u})$$

Fixing the network architecture to the optimal 5-layer, 50-neuron configuration, we evaluated the performance of different L_{physics} formulations. This evaluation demonstrated that the combination of the Pressure Poisson Equation (PPE) and the Continuity Equation (CE) achieved the lowest Mean Squared Error (MSE). Notably, applying the CE alone as a physical constraint was counterproductive, yielding an even higher MSE than the physics-uninformed baseline model. This result underscores a critical insight: the injudicious application of physical constraints in a PINN can degrade, rather than improve, predictive performance.

Table 3. Combinations of Governing equations

Governing Eqn	# of layers	# of neurons	MSE
CE	5	50	0.24
NSE & CE	5	50	0.16
PPE & CE	5	50	0.12
None	5	50	0.23

Therefore, our final optimized model for this study utilizes a 5-layer, 50-neuron architecture with a physics-informed loss term comprising the PPE and CE to ensure the highest predictive accuracy.

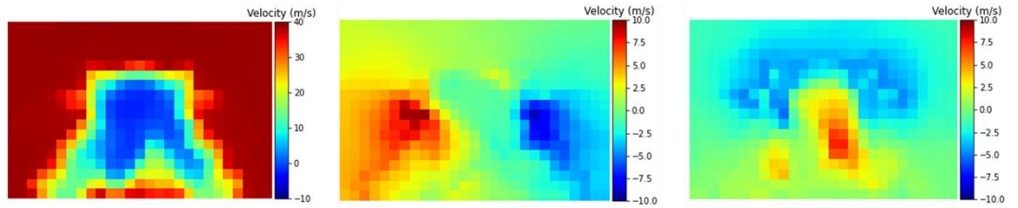
3.2 Analysis of predicted results

While Mean Squared Error (MSE) is a standard metric for regression, it offers limited physical insight into the accuracy of a predicted flow field. To provide a more robust and domain-specific evaluation, we assess the PINN’s performance by applying the Micro drag technique (Section 2.2) to the reconstructed wake. We then compare the drag coefficient (C_D) calculated from the PINN’s output with the ground truth C_D from CFD simulation. We define our success criterion as a discrepancy of less than 0.001 (1 count), which would validate the model’s practical utility for aerodynamic analysis.

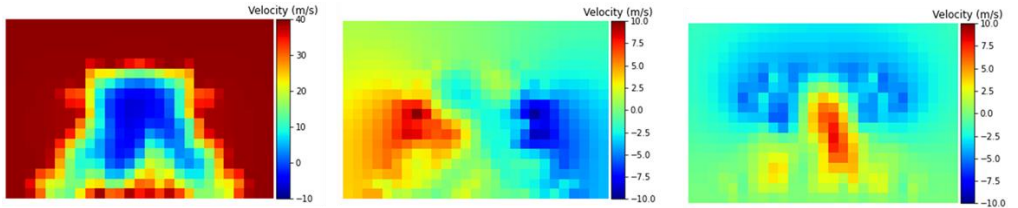
Figure 6. visually confirms the high fidelity of the reconstruction, comparing the PINN-predicted flow field in the $u \leq 10 \text{ m/s}$ zone with the ground truth. It is remarkable that the model achieved this accuracy without any direct training on the ground truth data within this unmeasurable region, relying solely on surrounding data and physical constraints.

A compelling quantitative comparison is presented in Figure 7., which shows Drag maps for three scenarios: the CFD ground truth, the PINN reconstruction, and the incomplete data mimicking the experimental measurements. The map from the incomplete data fails to capture the crucial drag recovery dynamics (the blue, $C_D < 0$ region), leading to a significant overestimation of the total drag coefficient ($C_D = 0.314$) versus the ground truth ($C_D = 0.294$). Conversely, the PINN-reconstructed map successfully reproduces the drag recovery region, resulting in a highly accurate drag coefficient of 0.295—a deviation of just 1 count from the ground truth.

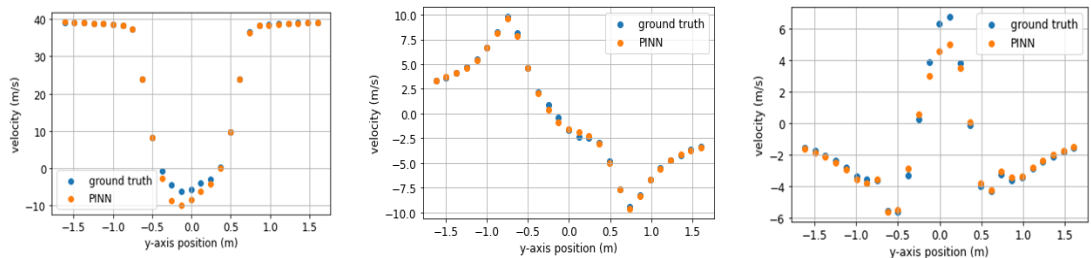
The excellent agreement, with the C_D difference falling well within our 1-count threshold, confirms that the PINN-based reconstruction is not only accurate but also robust enough for quantitative vehicle wake analysis.



(a) Predicted results by PINNs (u, v, w)

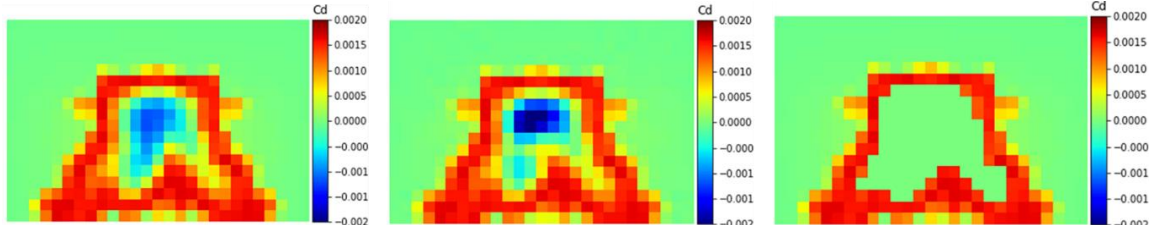


(b) ground truth (u, v, w)



(c) PINNs prediction vs. ground truth: velocity distribution in the $u < 10$ m/s region at $z=0.725$

Figure 6. PINNs results, ground truth's flow fields & velocity distribution



(a) ground truth

(b) reconstructed by PINNs

(c) Except $u < 10$ m/s

Figure 7. Drag map visualization

3.3 Case Study: Application to Real-World Wind Tunnel Measurements

Having validated our PINNs framework against high-fidelity CFD data, the next critical step was to prove its efficacy on real, incomplete experimental measurements. This section details a case study where the methodology was deployed during development of the new IONIQ 5 (PE), using sparse data gathered directly from wind tunnel test.

The primary engineering goal was to lower the vehicle's drag coefficient (C_D) to increase its All-Electric Range (AER). First, the original IONIQ 5 was evaluated in the wind tunnel. Our PINN model was then applied to its sparse wake measurements to reconstruct a complete flow field. The resulting drag map analysis (Fig8.) provided a crucial insight that was otherwise unobtainable from the raw data: an unusually weak drag recovery region. The quantitative assessment, enabled by our method, pinpointed the roof spoiler (white box) as the primary culprit, responsible for a substantial 18% of the total drag.

Armed with this direct, quantitative feedback from experimental data, engineers redesigned the spoiler for the new IONIQ 5. The modified vehicle was re-tested in the wind tunnel, and the PINN analysis was repeated. The new Drag map (Fig8.) confirmed the success of the modification: the drag contribution from the redesigned spoiler was dramatically reduced to approximately 3%. This case study showcases the framework's successful transition from a validation tool to a powerful diagnostic instrument in an active vehicle development program.

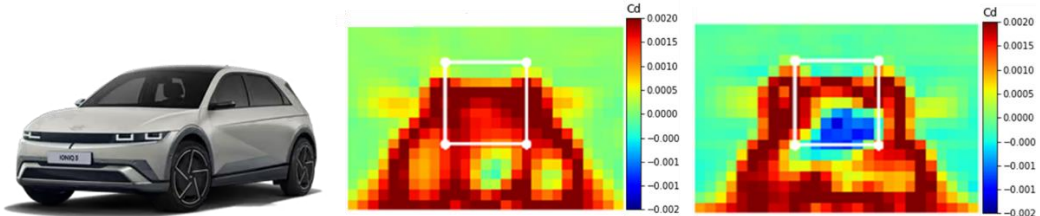


Figure 8. Drag map: IONIQ 5 (left), the new IONIQ 5 (right)

4 Conclusion

This study successfully developed a Physics-Informed Neural Networks (PINNs) framework capable of transforming incomplete, sparse wake measurements into complete, actionable flow fields. We initially validated the model's fundamental accuracy using a semi-synthetic CFD dataset of the DrivAer Estate model, optimizing it to a 5-layer architecture with a PPE-CE physics loss that predicted the drag coefficient to within 1 count (C_D 0.001).

Crucially, this research takes the vital step from validation in a controlled, simulated environment to successful application on real-world experimental data. To prove its practical readiness, the framework was applied directly to sparse data from a wind tunnel test of the new IONIQ 5. This PINN-driven analysis provided unprecedented quantitative insights, identifying a suboptimal roof spoiler as a major contributor to drag. The subsequent design improvements, guided by these findings, yielded a substantial drag reduction. This successful application on genuine experimental data validates our approach as a robust and impactful tool capable of bridging the gap between incomplete measurements and actionable engineering insights in the automotive development cycle. We anticipate that its capabilities can be further extended across diverse vehicle platforms by leveraging techniques like transfer learning.

5 Reference list

- [1] Kim, M., Lee, J., Kee, J., and Chang, J: Hyundai Full Scale Aero-acoustic Wind Tunnel, SAE Technical Paper 2001-01-0629, 2001
- [2] Heckmeier, Florian: Multi-Hole Probes for Unsteady Aerodynamics Analysis, Dissertation, Technical University of Munich, 2022
- [3] Juyong Jeong et al.: Data recovery of 2D Lifetime-Based Phosphor Thermometry Using Deep Neural Networks, Measurement Science and Technology, 2023
- [4] Dong Kim et al.: Sound Pressure Level Spectrum Analysis by Combination of 4D PTV and ANFIS method around automotive side view mirror models, Scientific Reports, 2021
- [5] M.Raissi, P.Perdikaris, G.E.Karniadakis.: Physics-informed neural networks: A deep learning framework for solving forward and inverse problems involving nonlinear partial differential equations, Journal of Computational Physics, 2019
- [6] A.Cogotti.: A Strategy for Optimum Surveys of Passenger-Car Flow Fields, SAE, 1989
- [7] A.I.Heft, T.Indiger, N.A.Adams.: Investigation of Unsteady Flow Structures in the Wake of a Realistic Generic Car Model, 29th AIAA Applied Aerodynamics Conference, 2011
- [8] Munson et al.: Fundamentals of Fluid Mechanics, Wiley